ELSEVIER

Journal of Hydrology 262 (2002) 68–83

Journal of Hydrology

www.elsevier.com/locate/jhydrol

Assessment of the long-term hydrologic impacts of Lake Nasser and related irrigation projects in Southwestern Egypt

Jeongkon Kim[1], Mohamed Sultan*

Environmental Research Division, Argonne National Laboratory, 9700 South Cass Avenue, Argonne, IL 60439-4843, USA

Received 1 March 2001; revised 14 January 2002; accepted 25 January 2002

Abstract

A two-dimensional groundwater flow model was constructed to investigate the long-term hydrologic impacts of Lake Nasser and the major land reclamation projects that use excess lake water in southwest Egypt. Egypt constructed (1964–1971) the Aswan High Dam, creating the Lake Nasser reservoir (length: 500 km; average width: 12 km) and is constructing the Tushka Canal to channel 5.0×10^9 m^3/yr of Lake Nasser water to reclaim 0.5×10^6 acres of desert lands. The model, constrained by regional-scale groundwater flow and near-lake head data, was successfully calibrated to temporal-observation heads from 1970 to 2000 that reflect variations in lake levels. Predictive analyses for the subsequent 50-yr period were conducted by employing the calibrated model. Simulations of long-term effects, beyond year 2000, of Lake Nasser on recharge and temporal groundwater head (base case scenario) show that recharge from the lake will continue at a much slower rate than during the 30-yr period of 1970–2000 (with approximately 86% reduction in 30-yr recharge). The modest projected pumping and injection activities in the study area are not expected to cause major deviation in the overall head distribution compared to the base case scenario. The investigation of effects of the new irrigation land development on the Nubian aquifer indicated that many of the proposed irrigation areas, especially those with small aquifer thickness, will become fully saturated with introduced water, resulting in potential flooding and salinization.

Keywords: Groundwater modeling; Nubian aquifer; Aswan high dam; Lake Nasser; Tushka canal

1. Introduction

Faced with overpopulation problems and a demand for development of new agricultural lands to support their increasing populations, Egypt and many of the world's arid and semi-arid countries have been adopting aggressive policies to develop and exploit their surface water resources. The environmental consequences of these major engineering efforts are too often overlooked. The Aswan High Dam, the second largest in the world, was erected as a multi-year storage scheme for Nile River water. The construction of the dam entailed the development of an extensive reservoir, designed to have a maximum water level of 183 m above sea level, a total capacity of 1.6×10^{11} m^3, a total length of 500 km, and an average width of 12 km (Said, 1993). Because the Lake Nasser reservoir has approached its maximum storage capacity in the past few years, the depressions west of Lake Nasser in the southwestern Desert of Egypt (Fig. 1) are currently being used as a natural flood diversion

* Corresponding author. Tel.: +1-630-252-1929; fax: +1-630-252-5498.

E-mail addresses: jkkim@lbl.gov (J. Kim), sultan@amoun.er.anl.gov (M. Sultan).

[1] Present address: Earth Sciences Division, Lawrence Berkeley National Laboratory, One Cyclotron Road, MS 90-1116, Berkeley, CA 94720, USA. Tel.: +1-510-495-2507; fax: +1-510-486-5686.

0022-1694/02/$ - see front matter
PII: S0022-1694(02)00013-6

Fig. 1. Moderate resolution imaging spectroradiometer satellite image acquired on February 19, 2000, showing the general physiographic features of Egypt, the study area, the Tushka canal, and the lakes to the west of Lake Nasser formed due to current high lake level.

basin to reduce possible downstream damage to the Nile valley caused by exceptional flooding.

Planning is under way to inject excess Lake Nasser water into the Nubian aquifer, and the Tushka Canal is being constructed (1998–2002) to divert 5.0×10^9 m^3/yr of excess Lake Nasser water to the Western Desert to increase agricultural land and also to alleviate overpopulation in the Nile valley and Nile delta. Under investigation is the construction of a network of canals to carry Nile water from one depression to another across the entire Western Desert (through the Kharga and Dakhla depressions; Fig. 1) after completion of the Tushka Canal.

All of these projects could have a profound effect

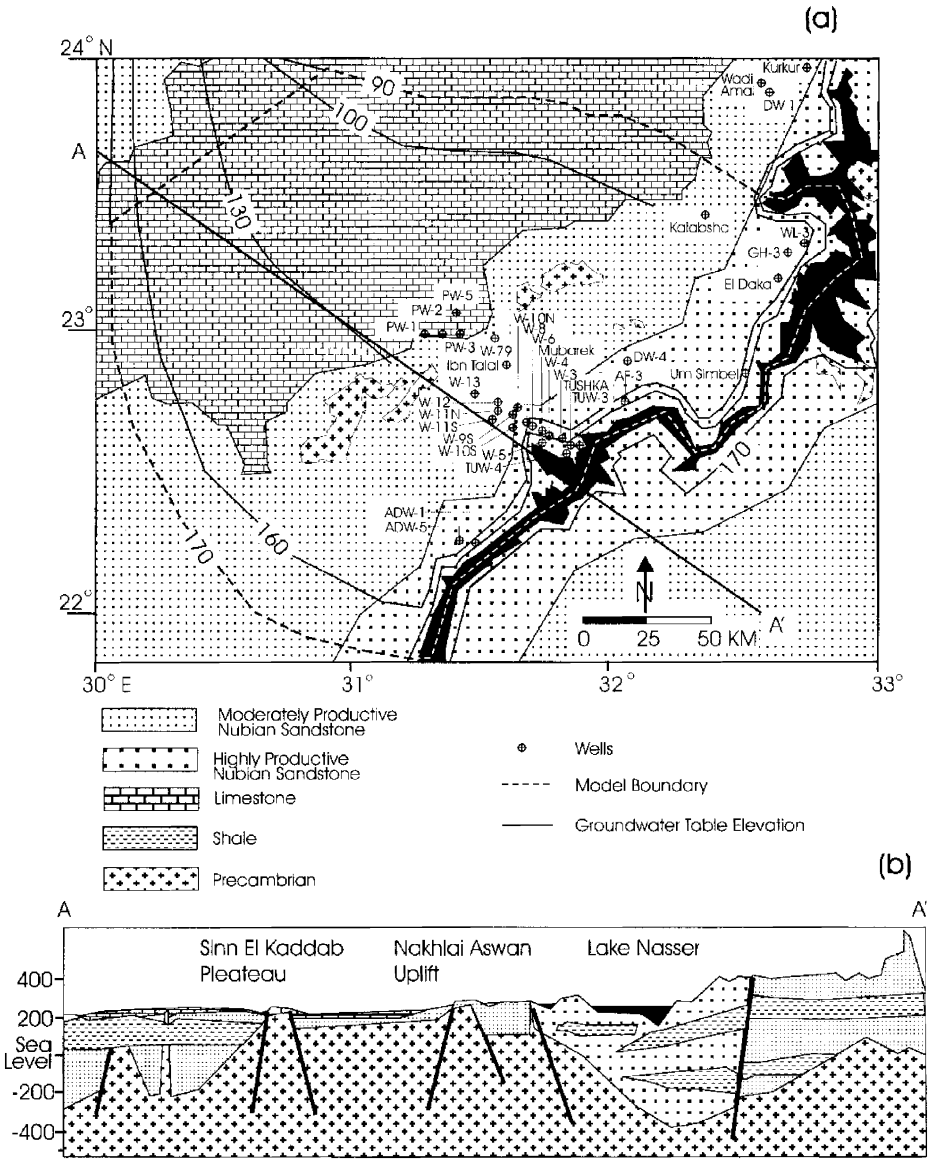

Fig. 2. Simplified hydrogeologic map for the study area. (a) Major hydrogeologic units, model boundaries, and locations of pumping and piezometric wells. (b) Northwest–southeast-trending schematic cross section along line A–A′ in panel (a).

on the groundwater level and water quality of the Nubian aquifer. This is one of the world's largest aquifers (covering 2.0×10^6 km^2 in Sudan, Libya, Chad, and Egypt, with reservoir capacity of 7.5×10^4 km^3; Hess et al., 1987), largely formed of the nonrenewable fossil groundwater recharged during previous, more humid climatic conditions that prevailed all over the present desert during the Quaternary (e.g. Sultan et al., 1997).

The objective of this study is to investigate the long-term hydrogeologic impact of the major engineering projects in Southwestern Egypt, namely the development of Lake Nasser, irrigation projects, and injection schemes. We developed a groundwater flow model by using MODFLOW (McDonald and Harbaugh, 1988), calibrated the model by employing observed head data for the

study area, and applied the model for prediction and sensitivity analyses.

2. Site description

The study area is largely covered by Neoproterozoic (550–900 Ma) crystalline igneous and metamorphic rocks (basement) of the Arabian-Nubian Shield (Sultan et al., 1990; Stern and Kroner, 1993) and Phanerozoic sedimentary rocks. The major stratigraphic units and the groundwater table level in relation to the water level in Lake Nasser are shown on the hydrogeologic map (Fig. 2a) and the schematic cross section (Fig. 2b) along line A–A′ in Fig. 2a. A number of features are apparent on the map and the cross section. The basement surface is uneven; it crops out near the lake in the northern part of the study area and along a major (300-km-long) uplift trending northeast–southwest, the Nakhlai–Aswan uplift, in the central part of the area. The basement surface forms an impervious lower boundary for the aquifer in the study area and acts as a barrier to lateral groundwater flow. The basement is unconformably overlain by Paleozoic and Mesozoic successions intercalated with minor shale layers of local extent and/or limited thickness. The lower part of the succession is made of undifferentiated conglomerate, sandstone, and shale (Gilf Formation) Paleozoic rocks that are encountered in wells drilled in the southern parts of the study area (e.g. ADW1, ADW5). The middle part of the succession is made of Abu Simbel Formation coarse pebbly sandstone, Abu Ballas fine sandstone and shale, and low-permeability El Borg Formation sandstone. All are of Upper Jurassic to Lower Cretaceous age. These materials are encountered in wells and in outcrops to the east of the uplift (e.g. W3, W4, W6, W8, W9S, DW4). The upper part of the succession, Nubia Formation sandstone, is exposed in the northern part of the study area (e.g. Kalabsha; RIGW, 1998b). West of the uplift, the Nubia Formation is overlain by karstified Tertiary limestone (e.g. Korkor, Garra, and Dungul Formations), locally capped by Dakhla shale and clay of the Upper Cretaceous age. Faulting is pronounced throughout the study area. Two major fault systems cut across the entire area, trending east–west and north–south. The former, the Kalabsha, is an active fault system. Because the shale layers are generally of local extent and limited thickness and because they are locally eroded or vertically displaced by extensive faulting, we assume the Paleozoic/Mesozoic aquifers in the study area to be unconfined.

Areas to the west of the uplift are composed largely of low-productivity aquifers with paleokarstified features, whereas areas to the east of the uplift are composed largely of highly to moderately productive aquifers, formed mainly of coarse- to medium-grained Paleozoic and Mesozoic sandstone with minor intercalations of shales (RIGW, 1998a). Both kinds of aquifers contain fossil groundwater that was recharged during wet paleoclimatic periods (RIGW, 1998a; Aly et al., 1993). However, areas east of the uplift could have received recent recharge from Lake Nasser (Abdel Karim, 1992). This suggestion is supported by the fact that the surface water level in Lake Nasser is generally higher than the groundwater level in these areas, as well as by the abrupt rise in groundwater level near the lake (Fig. 2a). Examination of groundwater level in the study area indicates a groundwater flow direction from southwest to northeast, consistent with the regional groundwater flow direction in the Nubian aquifer (Ball, 1927).

3. Model development and calibration

Our approach involves the development of a groundwater flow model through identification of model boundaries and initial conditions, then calibration of the model over a 30-yr period (1970–2000). We used the calibrated model to analyze the effects of the projected water management schemes for the period 2000–2050. Because the study area is mostly unconfined with relatively simple geologic settings (especially near the lake), a two-dimensional, unconfined groundwater flow model was found to be adequate for our modeling purposes. MODFLOW (McDonald and Harbaugh, 1988) was used to develop the model for the Nubian aquifer in the study area.

3.1. Model domain

The eastern, southern, northern, and western boundaries of the study area are bounded by Lake Nasser, latitude 22° 05′N–23° 50′N and longitude 30° 05′E, respectively (see Fig. 2a). The study region was discretized by using orthogonal grids of rows

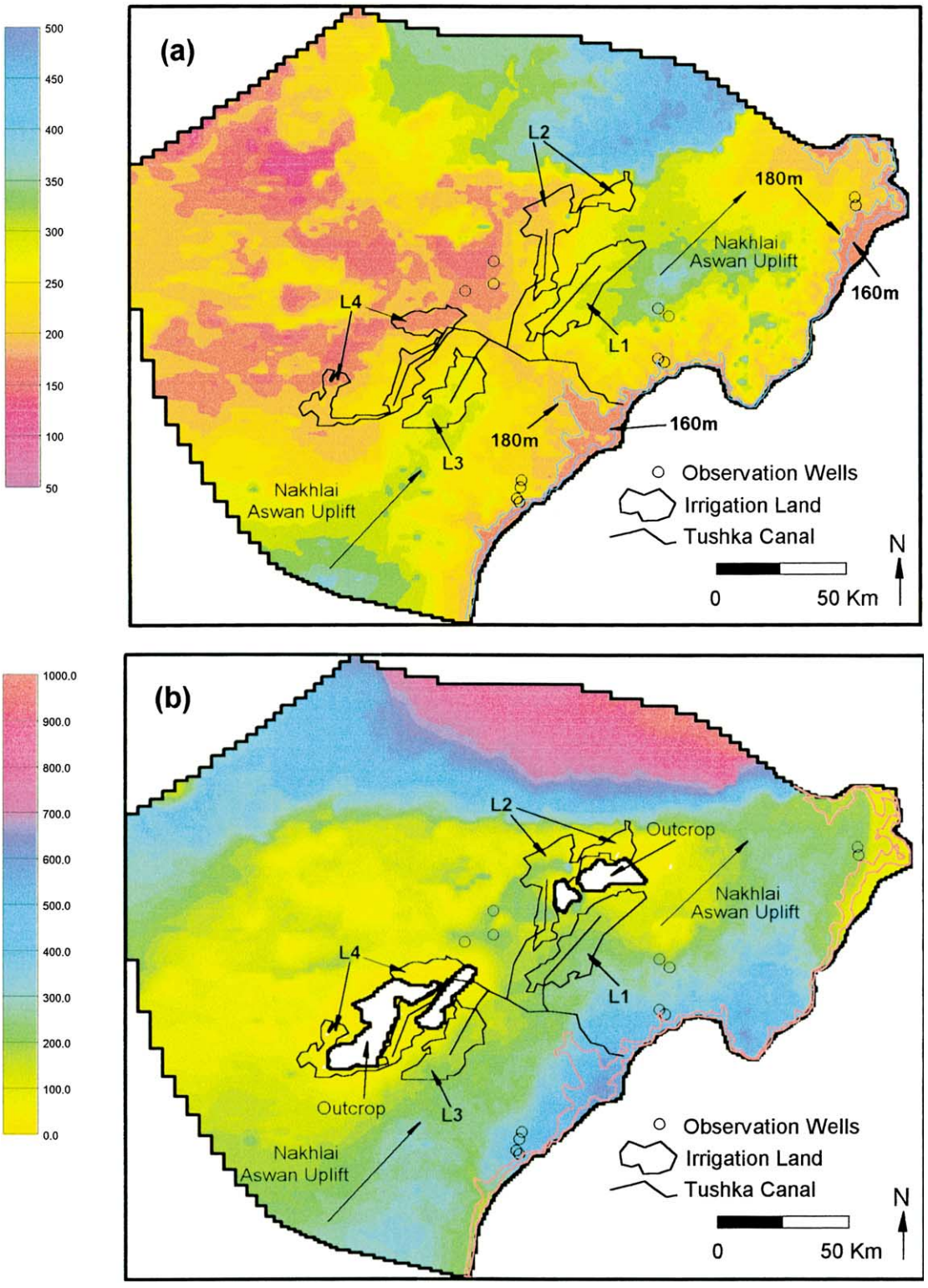

Fig. 3. Schematic map of the study area: (a) surface elevation; (b) aquifer thickness distribution; and (c) initial groundwater head distribution in the model.

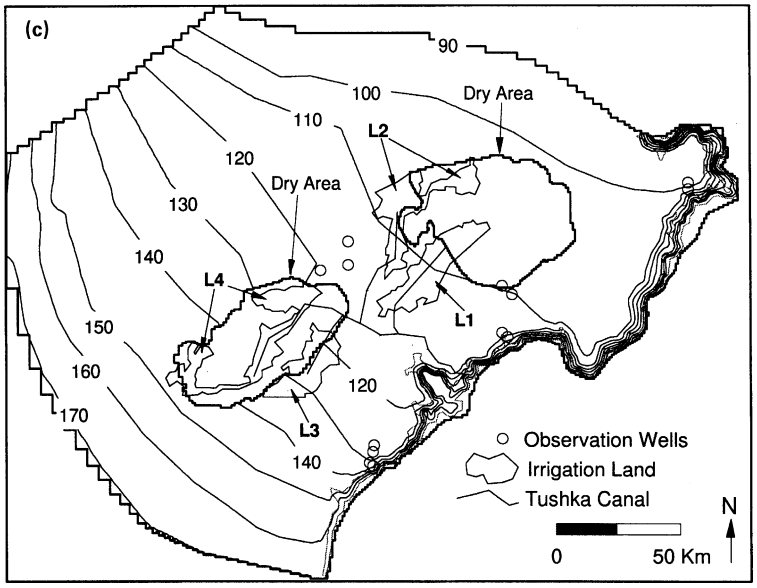

Fig. 3. (*continued*)

(251) and columns (288) varying in length between 0.5 and 5.0 km. Null properties were assigned to cells outside the model domain. The development and calibration of the model were conducted with the Groundwater Modeling System (GMS) developed by U.S. Department of Defense (DoD, 1998). The modeling area covers almost all of the existing pumping and monitoring wells, the Tushka Canal, and all of the proposed new irrigation localities.

Fig. 3a shows color-coded contours of the surface elevation obtained from 3-arc-second (approximately 85-m) Digital Terrain Elevation Data (DTED) prepared by the National Imagery Mapping Agency (NIMA, 1991). Inspection of Fig. 2a shows that the limestone plateau in the northern part of the study area and the northeast–southwest-trending Nakhlai–Aswan uplift constitute the highest (300–500 m above sea level) domains within the study area. The plateau and the uplift appear in shades of blue in Fig. 3a. The lowest areas are found along the lake shorelines and as a series of depressions that extend in northwest–southeast and northeast–southwest directions. Most of the areas to be cultivated (L1–L3, Fig. 3a) are on relatively high ground (250–350 m above sea level) and appear in shades of yellow on Fig. 3a. An exception is portions of area L4, at approximately 150 m in elevation; these are shown in shades of red on Fig. 3a.

The 1997 version of the hydrogeologic map of Egypt (El Saad El Ali sheet, scale 1:500,000; RIGW, 1998a) was used to extract the depth to the basement. The thickness of the aquifer was determined by subtracting the basement elevation from the surface elevation. Areas where the result of the subtraction was zero or less were interpreted as basement outcrops and were treated as inactive cells throughout the modeling. Fig. 3b shows color-coded contours of the thickness of the aquifer in the study area. In general, the predicted outcrops correlate well with observed outcrops shown in Fig. 2. As Fig. 3b shows, the thickness of the aquifer increases toward the lake, reaching 600 m at some locations. An exception is the northeastern part of the study area, where basement outcrops occur (shades of yellow). The thickness of the aquifer generally decreases from the lake toward the uplift and west of the uplift. The irrigation lands are generally underlain by thin aquifers, typically less than 50 m thick.

3.2. Initial and boundary conditions

The initial condition of the groundwater table distribution in 1970 was derived from the hydrogeologic map and observation data. Constant heads equal to the Nubian water table level were prescribed along

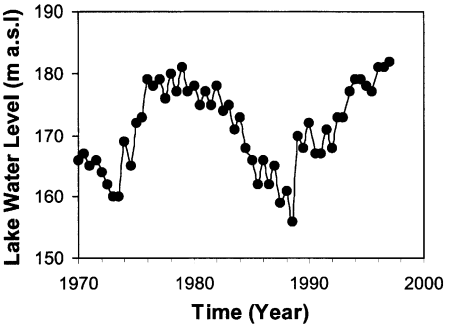

Fig. 4. Lake water elevation after RIGW (1998a).

the southern, western, and northern boundaries. The rationale for this type of boundary condition is the almost constant groundwater level over the past two decades along the boundaries. The eastern and south-eastern boundaries of our model were selected to coincide with the center of the lake. Fig. 3c shows the initial groundwater head distribution. The two main dry areas shown in Fig. 3c are generally characterized by high surface elevation (typically 200–400 m; Fig. 3a) and small aquifer thickness (<50 m; Fig. 3b). A considerable portion of the irrigation land falls within the dry areas.

Head-dependent flux boundary conditions were used to estimate recharge from the lake by employing the River Package module in MODFLOW (McDonald and Harbaugh, 1988). The River Package calculates flow to or from an adjoining groundwater system (the lake in this study) by using a linear function that depends on the difference in head between surface water and groundwater, along with a hydraulic conductance term for an individual active cell, as

$$Q = C(h_s - h_g), \tag{1}$$

where Q is the flow between the surface water system and the aquifer (positive for recharge into the aquifer), C is the hydraulic conductance of the lake bed, and h_s and h_g are the heads in the lake and at the bottom of the lake bed, respectively. The hydraulic conductance C for an individual active cell is given by

$$C = (K_l \times W \times L)/d, \tag{2}$$

where K_l is the average vertical hydraulic conductivity of the lake bed (L/T); W and L are the width and length of an individual cell, respectively; and d is the thickness of the lake bed sediments.

3.3. Model calibration

Transient flow simulations were required for model calibration over the calibration period from 1970 to 2000. The calibration was carried out by a trial-and-error fit of simulated groundwater heads to measured values. Calibration targets were established for the residual error statistics, and groundwater parameters were modified until the targets were satisfied. Data availability in the study area was generally limited. More wells are currently being drilled as the Tushka Canal project progresses. Luckily, the older wells (drilled in 1965–1980), though limited in number, are concentrated along the lake shoreline, where the interaction between the lake and the aquifer is most pronounced, enabling calibration of the model with confidence. Hydraulic conductivity values and yield coefficients of the aquifer materials and vertical hydraulic conductivity of the clay layer were the principal parameters varied during calibration. Because of the rare precipitation (EMA, 1996) and negligible pumping activities, largely restricted to pumping tests (Abdel Karim, 1992), precipitation and pumping were assumed negligible throughout the calibration. Anisotropy was also assumed negligible.

During the period of 1970–2000, the lake level fluctuated between 158 and 182 m. After construction of the Aswan High Dam in 1964, the surface water level in the lake rose from 121 m (above sea level) to 178 m in 1978. Subsequently, the lake level fluctuated, reflecting the intensity of the Nile inflows. Because of low Nile flows in the early 1980s (Said, 1993), the lake declined to its lowest level of 158 m in 1987, but the level started to rise again in the early 1990s, reaching 182 m by 1997 (Fig. 4). This latest rise in lake levels caused the Lake Nasser waters to overflow a spillway that was constructed to channel excess lake water and created four lakes to the west of Lake Nasser that are apparent on a satellite image acquired in February 2000 (Fig. 1). Fig. 3a shows predicted shoreline locations corresponding to lake levels of 160 and 180 m. The fluctuations of the lake level must have induced significant interactions between the lake and the aquifer, especially in the

Table 1
Stress periods used for model calibration

Stress period	Beginning (year)	Ending (year)	Duration (year)	Average lake level (m)	Average lake depth (m)
1	1970	1972	2	165.8	21.9
2	1972	1974	2	162.1	21.0
3	1974	1975	1	167.8	22.3
4	1975	1976	1	174.3	23.8
5	1976	1980	4	178.3	24.8
6	1980	1983	3	175.9	24.2
7	1983	1985	2	170.6	23.0
8	1985	1987	2	163.9	21.4
9	1987	1989	2	160.9	20.7
10	1989	1993	4	169.7	22.8
11	1993	1996	3	177.8	24.7
12	1996	2000	4	181.8	25.6

vicinity of the lake, triggered by the accompanying changes in head differences and lake area.

The calibration period was divided into 12 stress periods to effectively represent lake level fluctuations that affected recharge. Table 1 shows the length, average lake level, and average lake depth for each of the stress periods. The lengths of the stress periods were dictated largely by consistency in lake levels in consecutive years. The change in area was accounted for in the River Package by determining the inundated area for selected stress periods manually and then specifying head-dependent boundaries for cells corresponding to the inundated area. The lake areal extent was defined for every 5-m increment in lake stage from 160 to 185 m (i.e. 160, 165, 170, 175, 180, and 185 m) to account for the range of lake fluctuation from 1970 to 2000. For every 5-m increment of lake stage, cells in which lake stage exceeded surface elevation were specified as active cells for leakage computation.

The construction of the Aswan High Dam not only affected the surface and groundwater level in the area, but it also led to the development of appreciable deposits due to the settling of silt and clay layers as Nile River flow velocities were reduced. The thicknesses of these deposits range from tens of meters in northern Sudan to meters and less in the study area. An average thickness of 1 m was used for the clay layer in the study area (Said, 1993).

The hydraulic conductivity values that yielded the best calibration results are 4–35, 1.2, and 0.12 m/d for highly productive sandstone, moderately productive sandstone, and limestone, respectively. The calibrated values of hydraulic conductivity are within the ranges reported for the study area and surroundings (e.g. Abdel Karim, 1992; WPRP, 1998; Dasco, 1998a; Dasco, 1998b; RIGW, 1998b; RIGW, 1998c). The conductivity values are also consistent with those measured in the area and with published values for similar rock units elsewhere (Domenico and Schwartz, 1990). The calibrated vertical hydraulic conductivity of the clay layer, 8.6×10^{-3} m/d, falls within the range of reported values for similar sediments elsewhere (e.g. 5.96×10^{-4}–1.12×10^{-2} m/d; Harvey et al., 2000). The calibrated yield coefficients are 0.25, 0.25, and 0.15 for highly productive sandstone, moderately productive sandstone, and limestone, respectively.

Fig. 5 presents the calibration results. Observed versus computed heads at the observation wells in 1980 and 1990 are shown in Fig. 5a and b, respectively. Fig. 5c presents a time series of groundwater heads at four widely separated observation wells. Because the interactions between the lake and the aquifer will be most pronounced in proximity to the lake, we selected as our test wells GH7, AF3, and ADW1, which are near the northern, middle, and southern lake shorelines, respectively. For comparison, an additional well (PW3) that is distant from the lake was selected. Inspection of Fig. 5 shows a number of features. First, the flow model reasonably predicts the observed groundwater heads at the selected observation wells. Second, the elevated lake level caused the groundwater table to increase in the vicinity of the lake (e.g. GH7, AF3, and ADW1),

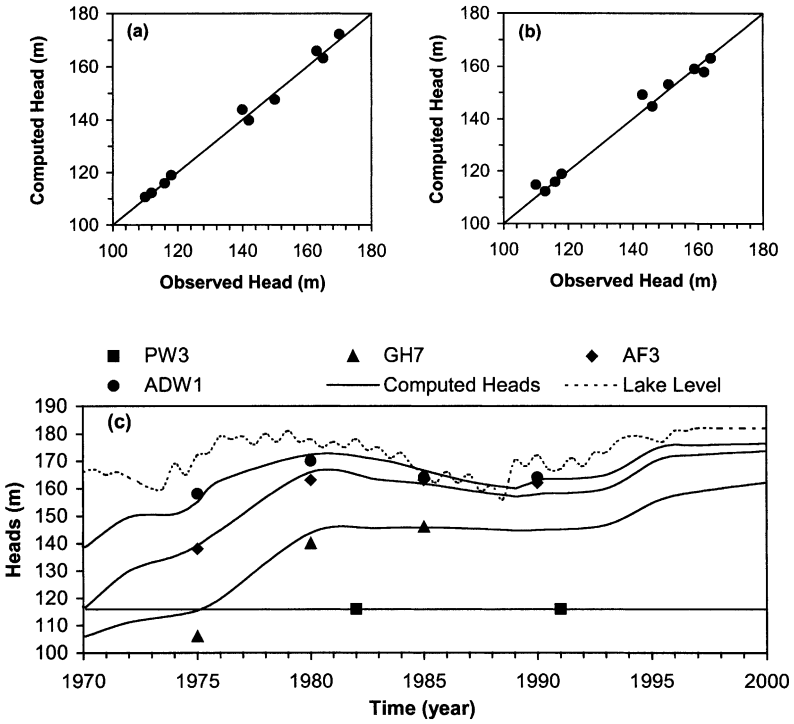

Fig. 5. Calibration results: (a) observed versus computed head at observation wells in 1980; (b) observed versus computed heads at observation wells in 1990; and (c) time series of groundwater head at four observation wells.

whereas the groundwater level remained constant in areas distant (>30 km) from the lake (e.g. well PW3). Third, the groundwater head at the observation wells in the vicinity of the lake reflected the lake stage fluctuation. For example, as lake level rose between 1975 and 1980, the groundwater level in wells ADW1 and AF3 rose by 26.7 and 17.2 m, respectively, and a drop in lake level between 1980 and 1989 was accompanied by a comparable drop in wells ADW1 (12.4 m) and AF3 (8.9 m).

4. Discussion and model application

4.1. Previous conditions after High Dam construction

Since the construction of the High Dam in 1965, the lake has been recharging the ambient Nubian aquifer. The High Dam has increased the lake levels and the inundated lake areas significantly. The groundwater table in the vicinity of the lake was significantly elevated because of recharge from the lake. The net recharge in the study area during the 30-yr calibration period was estimated to be 5.3×10^{10} m^3. The calibrated groundwater table distributions at selected time intervals of 1970, 1980, 1990, and 2000 are shown in Fig. 6a–d, respectively. The recharge from the lake increased the groundwater head within 30 km of the lake, but areas far from the lake (e.g. PW3) were not affected during the past 30 yr.

The advancement of the recharge front with time is manifested in Fig. 6 by a progressive widening in spacing between contour lines. For example, the front of the 120-m contour line continued to move away from the lake throughout the past 30 yr. The front advanced, in areas marked A, B, and C on Fig. 6, by 11, 11, and 3 km from 1970 to 1980; by 4, 4, and 3 km from 1980 to 1990; and by 2 km in each of the three locations between 1990 and 2000. The overall movement of the 120-m contour lines in areas A, B, and C was 17, 17, and 8 km, respectively, from the 1970 locations. The frontal movement in areas A and

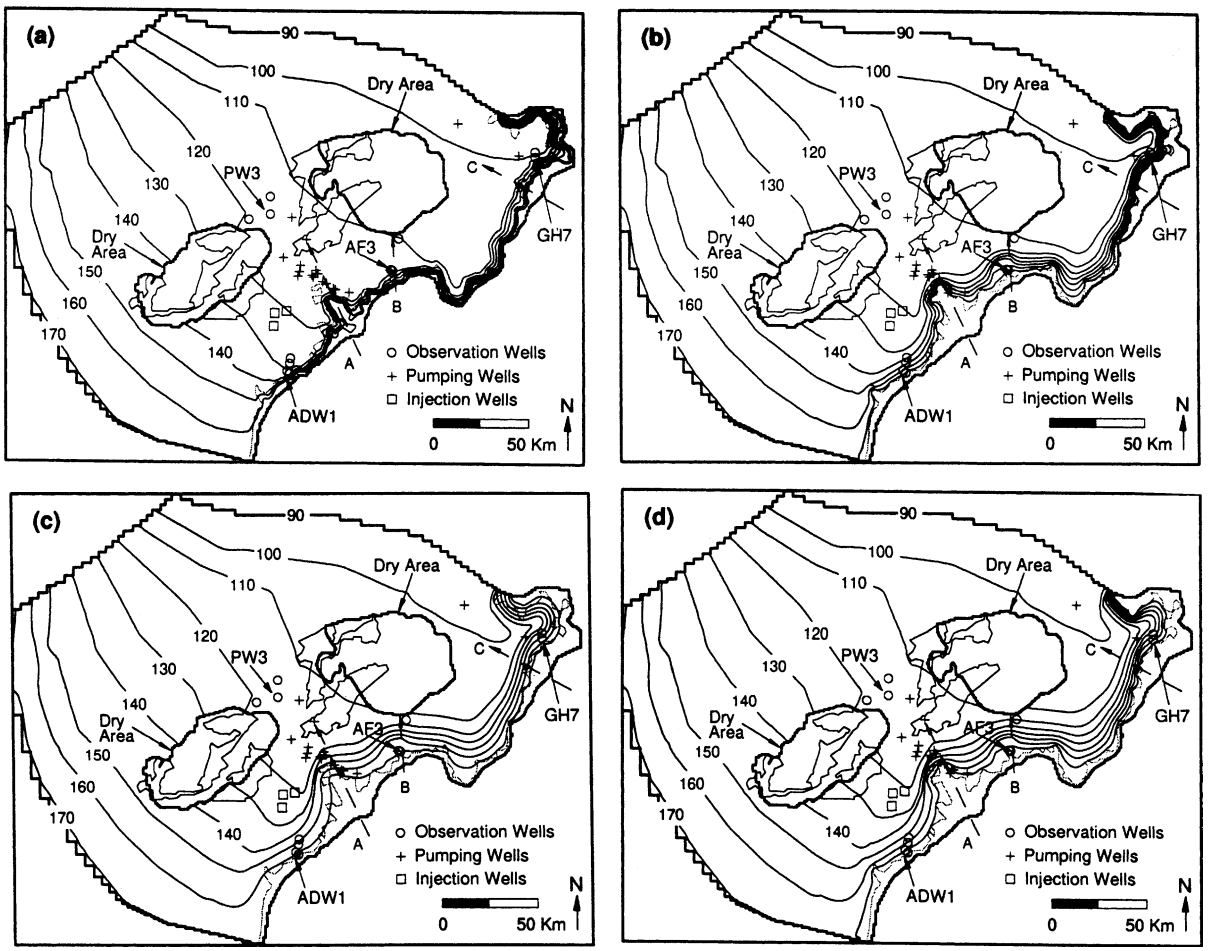

Fig. 6. Initial and calibrated groundwater head distributions: (a) initial (1970), (b) in 1980, (c) in 1990, and (d) in 2000.

B decreased as the front progressed into areas of relatively low hydraulic conductivity and into areas occupied by uplifts that act as a barrier to lateral groundwater flow (see Fig. 2). The decrease in potential difference between the lake and the aquifer also resulted in decreased recharge, thus reducing the recharge front movement. For example, the average movement rates in areas A, B, and C were 0.6, 0.6, and 0.2 km/yr, respectively.

The fluctuation of lake stage and the consequent change in the areal extent of the lake are reflected by contours close to the lake. For instance, the 160 m contour changed its direction (away from the lake or towards the lake) because of lake level fluctuations. Again, examination of the locations of the 160-m contours on the dotted arrows of A, B, and C (Fig. 6) shows that the net movements away from the lake from 1970 to 2000 were 10, 14, and 6 km, at A, B, and C, respectively.

4.2. Model applications

The calibrated model was used to analyze the effects of the projected water management projects for the period 2000–2050. The calibrated groundwater table distribution in the year 2000 (Fig. 6d) was used as the initial condition. The lake level increased nearly to full capacity in 1980, dropped to its lowest level in 1988–1989, rose again to its maximum level in 1998, and has remained at the maximum

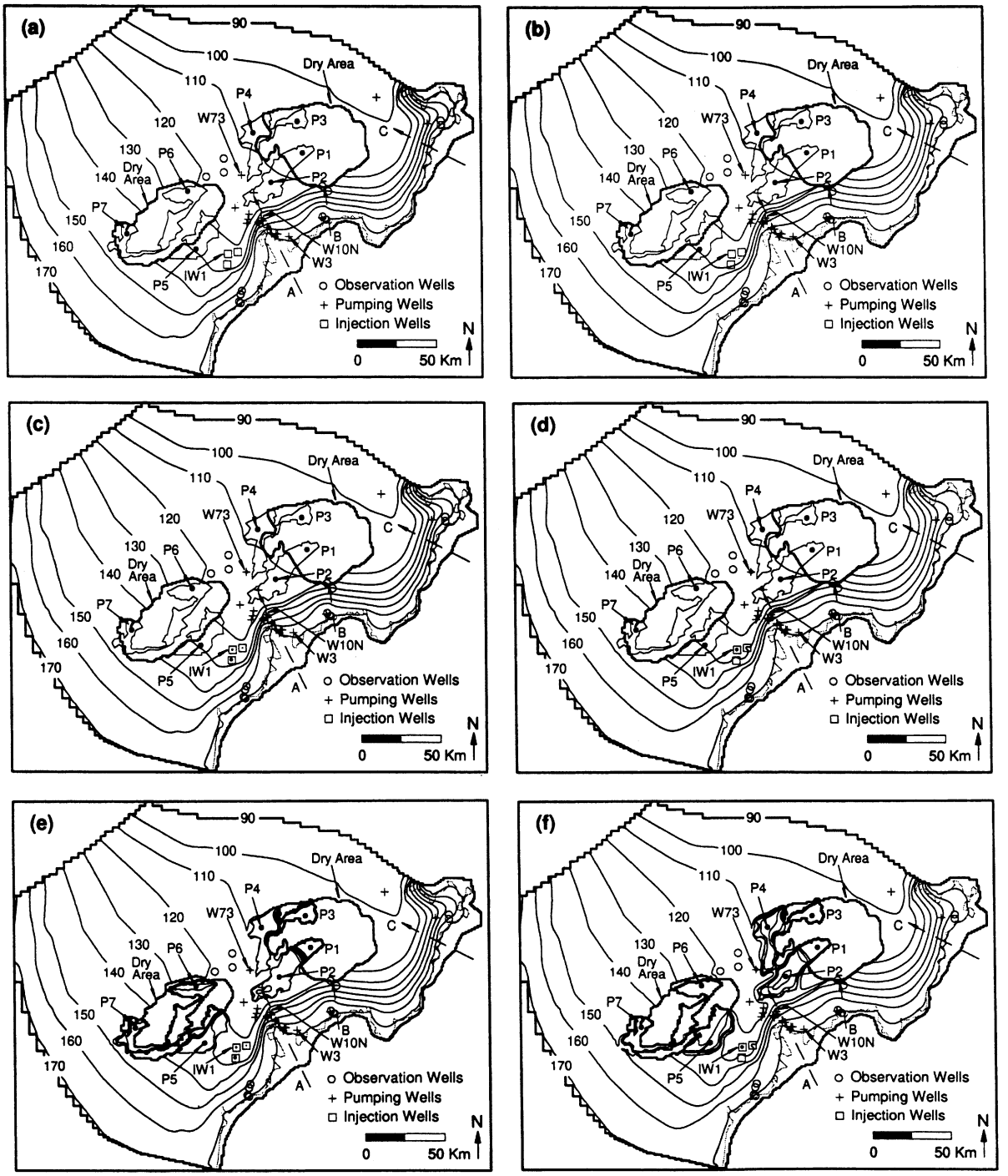

Fig. 7. Predicted groundwater head distributions: (a) in 2020 for Scenario 1, (b) in 2050 for Scenario 1, (c) in 2020 for Scenario 2, (d) in 2050 for Scenario 2, (e) in 2020 for Scenario 3, and (f) in 2050 for Scenario 3.

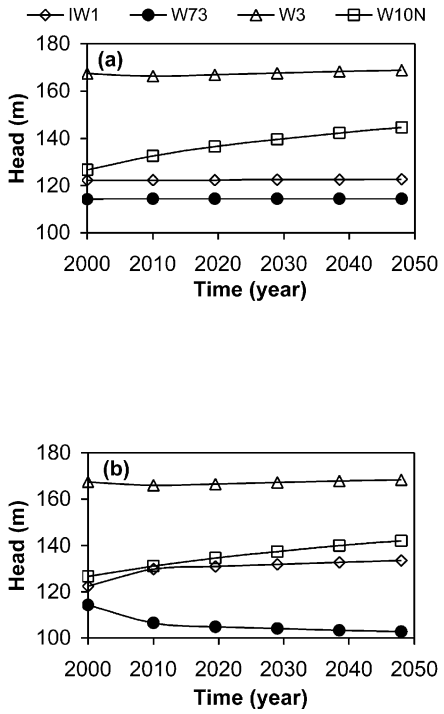

Fig. 8. Changes in groundwater head at selected pumping and injection wells. (a) Scenario 1 and (b) Scenario 2.

level until the present time (Fig. 4). In our simulations, we adopted the average lake level (172.8 m) for the past 20 yr to account for the historical lake level course after the lake was filled with water in 1980. Sediments upstream of the study area are relatively thick and irregular, reaching 25 m in thickness. In contrast, the clay layer downstream in our study area is typically thin (1 m or less) and generally uniform in thickness (Said, 1993). These differences are attributed to rapid river flow upstream versus gentle flow downstream. Because of the absence of detailed sediment thickness profiles across the lake in the study area, we assumed constant thickness and hydraulic conductivity for the sediment layer in this area. These assumptions are probably reasonable, given the success we had in matching the observed and simulated regional head data. Locally, these assumptions could lead to overestimation or underestimation of recharge from the lake.

Because of the recharge fronts found to propagate from the lake toward the dry area and the irrigation recharge in the dry area in Scenario 3, wetting of cells was allowed in the three scenarios according to the criterion of McDonald et al. (1991), as

$$h = bot + WETFCT(THRESH), \quad (3)$$

where h is the head at a cell that becomes wet, *bot* is the bottom elevation of the cell, and *WETFCT* is the wetting factor. Because of the high nonlinearity caused by the steep geometry of the bottom elevation in the initially dry areas of the planned irrigation lands, simulations required large numbers of iterations and often failed to converge, especially in Scenario 3 (below). A number of trial-and-error simulations were conducted to overcome the convergence problem. The best results were obtained when *WETFCT* was between 0.01 and 0.03, with a maximum of 50 iterations.

We considered three scenarios to systematically examine the effects of different stresses to the aquifer:

- Scenario 1: Recharge from lake (base case, continuation of 2000 conditions)
- Scenario 2: Base case, plus pumping and injection
- Scenario 3: Base case, plus pumping and injection, plus irrigation recharge

4.2.1. Scenario 1

Scenario 1 was simulated to investigate long-term changes of groundwater head in response to recharge from the lake without other natural or artificial stresses to the system. Scenario 1 is considered a baseline condition against which results for other scenarios can be compared. It has been more than 30 yr since the High Dam was erected. The construction of the High Dam resulted in elevated lake levels, expanded lake areas, and increased aquifer recharge from the lake. The groundwater table in the vicinity of the lake ($<$30 km) was significantly elevated by the recharge. Over time, the recharge from the lake to the aquifer must have been decreasing significantly. However, recharge from the lake is expected to continue. Further, the record lake levels for the past 3 yr made it important to predict the rate and the extent of groundwater recharge beyond the current condition before other water resource management plans are actually implemented.

Simulation results for Scenario 1 indicate a significant decrease in recharge from the lake to the aquifer,

as expected. For example, a comparison of the total net recharge for 30 yr, from 2000 to 2030, with that during the calibration period of 1970–2000 shows an 86% reduction. Continued recharge (1.5×10^{10} m^3 for 50 yr from 2000 to 2050), however, is expected to result in elevated groundwater tables, as shown in Fig. 7a and b, which present groundwater head distributions in 2020 and 2050, respectively, for Scenario 1. Comparison of Fig. 7a and b with Fig. 6d clearly shows, for example, that the recharge front of the 120-m contour is continuously advancing northwestward. Fig. 8a shows expected head changes at wells selected to monitor the effect of recharge at different locations (see Fig. 7 for exact locations of the selected wells). The groundwater head is constant for wells that remain distant from the advancing lake front (e.g. W73; Figs. 7 and 8) and for wells that are located close to the lake and have therefore apparently nearly reached steady-state conditions. Heads change considerably for wells in proximity to rapidly advancing fronts (e.g. W10N, W3), which are characterized by a steep head gradient (tight contours). Changes in groundwater head at W3, IW1, and W73 will be less than 1% for the next 50 yr, while groundwater heads at W10N will increase by 14%. Because the agricultural areas are topographically higher than the advancing front (compare Fig. 3a with Fig. 7a and b), we conclude that the rise in groundwater levels resulting from the advancing recharge front would pose no flooding risks for these areas.

4.2.2. Scenario 2

Scenario 2 was simulated to assess the impacts of pumping at wells around the canal as part of the Tushka Canal project and the effects of injecting excess lake water into the aquifer. The Egyptian Government plans to implement a number of management scenarios to maximize the water resources available in Lake Nasser. Besides the new irrigation land development in the Tushka depression area, the excess water in the lake will be recharged to the Nubian aquifer via injection wells, as shown in Fig. 6. In addition, some water from the Nubian aquifer will be extracted in wells around the canal (Fig. 6). The predicted pumping rates (e.g. WPRP 1998; MPWWR, 2000) for all 16 wells in the vicinity of the Tushka Canal and for the remaining three wells (El Sebouh, Gerf Hussein, and Kalabsha) are 500,000 and 1,090,000 m^3/yr, respectively, and injection rates were assumed to be 1,000,000 m^3/yr for three injection wells. The Egyptian Government is still in the exploration phase of the injection project. The locations of our injection wells approximate the location of the experimental injection site.

Fig. 7c and d present the impacts of pumping and injection in the years 2020 and 2050 in Scenario 2. The overall distribution of the regional groundwater table in this scenario is similar to that for Scenario 1. However, pumping and injection at scattered wells result in the localized development of cones of depression and groundwater mounds as shown in Fig. 8b at the selected wells (e.g. W73 for depression; IW1 for mound). For the simulated pumping rates described earlier, the drop in groundwater level is balanced by recharge at the wells near the lake (e.g. W3, W10N). The groundwater head changes at W3 and W10N will be reduced by 2% or less in 2050, compared to the results for Scenario 1. Well W73 will experience a head decrease of about 10% due to pumping, whereas the groundwater head at IW1 will increase by about 9% due to injection of 1,000,000 m^3/yr for 50 yr. Recharge from the lake in Scenario 2 was increased by 1% over that in Scenario 1. Because the projected pumping and injection activities in the study area are modest, we foresee no major deviation in the overall head distribution from that presented in Scenario 1. Only local cones of depression or mounds will result.

4.2.3. Scenario 3

Scenario 3 was designed to investigate the effects of new irrigation land development, in conjunction with pumping and injection, on the Nubian aquifer. The construction of the Tushka Canal started in 1998 and is scheduled to be completed by 2002. Shortly after that, irrigation and land development will commence in the Tushka depression. Lake water will be supplied for cultivation in the planned irrigation area of 2.2×10^4 km^2. Crops that will be cultivated include palm trees, medicinal plants, potato, sesame, and vegetables (MPWWR, 1997; Altorkomani, 1999). In arid areas like the Tushka area, approximately 1.0, 0.5, and 0.9 m^3/yr m^2 are required for spraying, dripping, and surface canal irrigation methods, respectively (Altorkomani, 1999). We assumed that the dripping method, which minimizes evaporation loss, is likely to be selected.

Table 2
Variation in water table level at selected locations within irrigation lands (Scenario 3, 2000–2050)

Location	Water table level in year indicated (m)					Surface elevation (m)	Aquifer thickness (m)
	2010	2020	2030	2040	2050		
P1	201.8	209.6	217.3	224.9	232.4	277.1	83.3
P2	120.0	128.0	135.9	143.7	151.1	268.3	207.4
P3	212.5	221.9	231.1	240.0	248.5	234.5	31.0
P4	116.3	124.3	132.0	139.6	147.1	187.6	183.2
P5	137.2	145.2	153.2	161.0	168.7	285.5	177.9
P6	154.4	162.5	170.6	178.8	187.2	161.5	15.1
P7	170.5	178.8	187.1	195.4	203.5	172.2	10.0

The estimated water losses due to evaporation and evapotranspiration from the Western Desert oases could reach 0.2 and 0.1 m/yr, respectively (Altorkomani, 1999). The net recharge from the irrigation development was assumed to be 5.5×10^{-4} m/d (0.2 m/yr). Many of the proposed areas are dry because of the relatively high elevation of the base of the aquifer in these areas (Fig. 3c), and depths to the base of the aquifer measured from ground surface in many of the planned irrigation areas are shallow (Fig. 3b). Therefore, special attention was given to determine whether infiltration due to irrigation could cause flooding in the study area.

Fig. 7e and f presents groundwater head distributions in 2020 and 2050 for Scenario 3. In this scenario, the groundwater table distributions are quite different from those in Scenarios 1 and 2. The previously dried portions of the proposed irrigation areas become saturated with the introduced water, form groundwater mounds, and connect to the surrounding aquifer. Such major changes in groundwater table due to irrigation development will affect and complicate the distribution and movement of groundwater in the vicinity of the proposed irrigation areas (Fig. 7e and f). Large segments of the irrigation lands that were originally identified as dry lands (areas originally devoid of groundwater head contours in Fig. 6a–d) become wet and develop groundwater head contours (Fig. 7e and f). Dry areas were identified earlier as characterized by small aquifer thickness. Our simulations show that these areas could be subject to flooding, given the speedy rise in groundwater level expected in areas with shallow impervious basement, where the groundwater head might rise above the ground surface because of irrigation recharge. Table 2 shows head information (2010–2050) for seven locations (P1–P7) with various aquifer thickness within the irrigation lands. By 2020, both P7 and P6, the locations with the smallest aquifer thickness ($<$15 m), will be flooded (Fig. 7e). Similarly, P3, with an aquifer thickness of 31 m, will be flooded by the year 2050 (Fig. 7f). All remaining locations will witness a rise in groundwater table, yet because of their relatively larger aquifer thickness, flooding will not pose a risk within the next five decades. Given the shallow depth of the basement (typically 10–50 m) under the new cultivation lands, the projected rise in groundwater could pose salinization and possibly flooding problems. Additional careful, systematic investigations are advised before implementation of the irrigation projects.

5. Sensitivity analyses

A series of analyses was conducted to investigate the sensitivities of recharge and water table increase in and around the irrigation lands to lake level and irrigation infiltration rate, respectively. Only one parameter of interest was varied in each analysis, holding all other conditions of the simulation constant. Effects of sensitivity cases are discussed in terms of total recharge and expected flooding times for the lake level and the irrigation infiltration rate, respectively.

Recharge is sensitive to certain key parameters through the interactions between lakes and the aquifer, with the major parameters being lake level, the thickness and vertical hydraulic conductivity of clay deposits, and the movement of groundwater in the aquifer. In Scenario 1, we assumed an average lake level (172.8 m) obtained by averaging the lake levels during a 20-yr period from 1980 to 2000. To represent

a maximum recharge case, we conducted a sensitivity analysis by assuming that the lake level remains unchanged after the year 2000 at 182 m, which is 1 m short of the maximum permissible water level behind the High Dam (Said, 1993). This assumption might be reasonable, given the progressive decrease in discharge from the lake with time (see Section 5) and the peak lake level records maintained throughout the past 3 yr (Fig. 4). In fact, it was these unexpected peak lake levels that motivated the Egyptian Government to launch the Tushka Canal project. Raising the lake level to 182 m, which is 9.2 m above the base case lake level of 172.8 m, yields an increase of 184% in net recharge, as measured in year 2030. However, the difference decreases progressively to 112% in year 2050.

An analysis of the sensitivity of groundwater table increases to the irrigation recharge rate was conducted by increasing the recharge rate in the planned irrigation lands to 5.48×10^{-3} m/d (twice the rate used in Scenario 3). Locations P6 and P7 (with the small aquifer thickness of <15 m) and location P3 (31 m) will be flooded before year 2010 and year 2020, respectively. The increased irrigation recharge is expected to decrease the flooding time at P3 by 20 yr compared to Scenario 3. Remaining locations are not expected to be subject to flooding because of their relatively larger aquifer thicknesses, even under the condition of increased irrigation recharge.

6. Summary and conclusions

A two-dimensional groundwater flow model was used to investigate the long-term hydrologic impacts of the development of Lake Nasser and the major land reclamation projects currently under way in southwest Egypt. The model, constrained by regional-scale groundwater flow and near-lake head data, was calibrated to temporal-observation heads from 1970 to 2000. The calibrated results show good agreement with observed transient heads, which reflect variation in lake level. The estimated net recharge from the lake in the study area between 1970 and 2000 is 5.3×10^{10} m^3. Results further indicate that the maximum front advance, as measured by the 120-m water table perpendicular to the lake shoreline, was <20 km by year 2000 (approximately 0.6 km/yr).

Predictive analyses for the next 50-yr period were conducted by employing the calibrated model. The results for the baseline scenario (long-term temporal groundwater head changes in response to recharge from the lake, without other natural or artificial stresses to the system) show that recharge from the lake will continue, but at a much slower rate than during the previous 30-yr period (approximately 86% reduction in 30-yr recharge). The simulation results for pumping and injection around the canal indicate that the modest projected pumping and injection activities in the study area will not cause major deviation of the overall head distribution from the base case, though some local cones of depression and groundwater mounds are expected. The results for Scenario 3, designed to investigate effects on the Nubian aquifer of developing the new irrigation land, in addition to pumping and injection, indicate that the irrigation development will complicate the distribution and movement of groundwater in the vicinity of the proposed irrigation areas. In particular, many proposed irrigation areas with small aquifer thicknesses that were previously dry will become saturated with introduced water. The heads in those areas will continue to increase, resulting in potential flooding and salinization.

Research is under way to investigate the effects of land use and land cover (LULC) changes on water cycle and carbon sinks in the arid parts of the world. Groundwater flow modeling studies similar to that presented here should be useful in combination with geochemical and biological studies on water and soil samples for understanding the interplay between LULC changes and the water cycle and carbon sinks.

Acknowledgements

We thank Professors Mofeed Shehab, Farouk Ismail, Naguib El Helaly, Fathy Saad, Hamdy Ibrahim, and Zeinhom El Alfy for facilitating collaborative scientific research between Cairo University and Argonne National Laboratory. This study at Argonne National Laboratory was supported by NASA's Land Cover Land Use Change Program and by Cairo University through U.S. Department of Energy contract W-31-109-Eng-38.

References

Abdel Karim, M.H., 1992. Hydrogeological characteristics of groundwater aquifer at Lake Nasser region. MSc thesis. Cairo University, Giza, Egypt.

Altorkomani, G., 1999. The Geomorphology of Tushka and Development Potentialities. Geographical Research Series, vol. 4. The Egyptian Geographical Society, Cairo (in Arabic).

Aly, A.M., Froehlich, K., Nada, A., Awad, M., Hamza, M., Salem, W.M., 1993. Study of environmental isotope distribution in the Aswan High Dam Lake (Egypt) for estimation of evaporation of lake water and its recharge to adjacent groundwater. Environmental Geochemistry and Health 15, 37–49.

Ball, J., 1927. Problems of the Libyan desert. Geographical Journal 70, 21–38, 105–128.

Dasco, 1998. Lithology and casing details for well no 3. Ministry of Public Works and Water Resources, National Egyptian Drilling and Petroleum Services Co., Cairo.

Dasco, 1998. Lithology and casing details for well no 13. Ministry of Public Works and Water Resources, National Egyptian Drilling and Petroleum Services Co., Cairo.

DoD, 1998. Groundwater Modeling System (GMS), Version 2.1. U.S. Department of Defense, Washington, D.C.

Domenico, P.A., Schwartz, F.W., 1990. Physical and Chemical Hydrogeology. Wiley, New York.

EMA, 1996. Climatic Atlas of Egypt. Egyptian Meteorological Authority, Ministry of Transport and Communications, Cairo.

Harvey, F.E., Rudolph, D., Frape, S.K., 2000. Estimating groundwater flux into large lakes: application in the Hamilton harbor, western Lake Ontario. Groundwater 38 (4), 550–556.

Hess, K.-H., Hissene, A., Kheir, O., Schnacker, E., Schneider, M., Thorweihe, U., 1987. Hydrogeological investigations in the Nubian aquifer system, Eastern Sahara. In: Klitzsch, E., Schrank, E. (Eds.). Research in Egypt and Sudan. Von Dietrich Reimer, Berlin, pp. 397–464.

McDonald, M.G., Harbaugh, A.W., 1988. A modular three-dimensional finite difference groundwater flow model. USGS Techniques of Water Resources Investigations, Book 6. U.S. Geological Survey, Reston, VA.

McDonald, M.G., Harbaugh, A.W., Orr, B.R., Ackerman, D.J., 1991. A method of converting no-flow cells to variable-head cells for the U.S. Geological Survey modular finite-difference ground-water flow model. U.S. Geological Survey Open-File Report 91-536.

MPWWR, 1997. Preliminary evaluation of the project for the development of the South Valley. Ministry of Public Works and Water Resources, Cairo.

MPWWR, 2000. Data on the Productive Wells Drilled in the Tushka Area. Ministry of Public Works and Water Resources, Executive Branch for Tushka Canal Project, Tushka, Egypt.

National Imagery Mapping Agency (NIMA), 1991.

RIGW, 1998. Hydrogeological map of Egypt, El Saad El Ali Sheet, Scale 1:500,000. Research Institute for Groundwater, Academy of Scientific Research and Technology, Cairo.

RIGW, 1998. Technical Report for Well Kalabsha. Research Institute for Groundwater, Cairo.

RIGW, 1998. Technical Report for Garf Hussein. Research Institute for Groundwater, Cairo.

Said, R., 1993. The River Nile: Geology, Hydrology, and Utilization. Pergamon Press, New York.

Stern, R.J., Kroner, A., 1993. Late Precambrian crustal evolution in northeast Sudan: isotopic and geochronologic constraints. Journal of Geology 101, 555–574.

Sultan, M., Chamberlain, K.R., Bowring, S.A., Arvidson, R.E., Abuzied, H., El Kaliouby, B., 1990. Geochronologic and isotopic evidence for involvement of pre-pan-African crust in the Nubian Shield, Egypt. Journal of Geology 18, 761–764.

Sultan, M., Sturchio, N., Hassan, F.A., Hamdan, M.A.R., Mahmood, A.M., El Alfy, Z., Stein, T., 1997. Precipitation source inferred from stable isotopic composition of Pleistocene groundwater and carbonate deposits in the Western Desert of Egypt. Quaternary Geology 4, 29–37.

WPRP, 1998. Hydrogeology of Deep Aquifers in the Western Desert and Sinai. Ministry of Public Works and Water Resources, Water Policy Reform Program, Cairo.